

Supporting Documents

Figure S1-a, Traces A, B, and C illustrate ATR FT-IR spectra of p(EEMA) and p(AcrNPP) homopolymers, and p(AcrNPP/EEMA) copolymer, respectively. As seen in Trace A, characteristic bands of p(EEMA)^{1, 2} at 1730 (C=O, ester) and 1120 (C-O-C asym str) cm^{-1} are detected. Trace B illustrates the IR spectrum of p(AcrNPP) with the characteristic bands³⁻⁸ at 2961 (CH_3 asym str), 2931 (CH_2 asym str), 2875 (CH_3 sym str), cm^{-1} in the C-H stretching region as well as the 2820-2760 (N- CH_2), 1642 (C=O, amide I), 1445 (C-H def), and 1050-980 (ring skeletal vib) cm^{-1} bands. Trace C illustrates IR spectrum of p(AcrNPP/EEMA) copolymer. As anticipated, the selected bands in the 3000-2850 cm^{-1} region and the 1445 cm^{-1} band due to the C-H stretching and CH_2/CH_3 deformation modes overlap between the p(EEMA) and p(AcrNPP), but the characteristic band at 1730 cm^{-1} due to the carbonyl ester of EEMA as well as the bands at 2820-2760, 1642, and 1050-980 cm^{-1} due to the $>\text{N-CH}_2$ tertiary amines, amide groups, and the ring structure of AcrNPP are observed, thus confirming copolymerization. Further evidence of copolymerization is illustrated in ^1H NMR spectrum of p(AcrNPP/EEMA) recorded at 22 $^\circ\text{C}$ in CDCl_3 shown in Figure S1-b. The resonances at 1.1 (-C- CH_3), 1.2 (-O- CH_2 - CH_3), 3.4-3.5 (- CH_2 -O- CH_2 -), and 4.05 (-COO- CH_2) ppm arising from the copolymerization of EEMA units^{2, 6-8} are detected, and the peaks at 0.92 (- CH_2 - CH_3), 2.2 ($>\text{N-CH}_2$ -), 2.3-2.5 (-N-(CH_2)₂), and 3.5-3.6 (-CO-N-(CH_2)₂) ppm due to the AcrNPP units^{3, 5-8} are also present. The resonance at 7.23 ppm is due to CDCl_3 solvent. These spectroscopic data demonstrate that AcrNPP and EEMA monomers are copolymerized with the feed ratio of 1:1 during free radical semicontinuous copolymerization. The copolymerization yield

was 82 % and the copolymer composition determined from ^1H NMR experiments was AcrNPP/EEMA=0.52/0.48.

Figure S2 illustrates TEM images of p(AcrNPP/EEMA) and p(DMAEMA/nBA). As seen, p(AcrNPP/EEMA) colloidal particles exhibit more homogenous morphology compared to p(DMAEMA/nBA), which is attributed to the increased solubility and polarity of EEMA resulting from the presence of ether linkages. Since AcrNPP and EEMA exhibit similar affinities to polymerize within the micelles, the particles morphologies are more homogenous (A). In contrast, when nBA is copolymerized with DMAEMA, hydrophobic nBA will polymerize first, followed by DMAEMA, thus resulting in a heterogeneous shell (B).

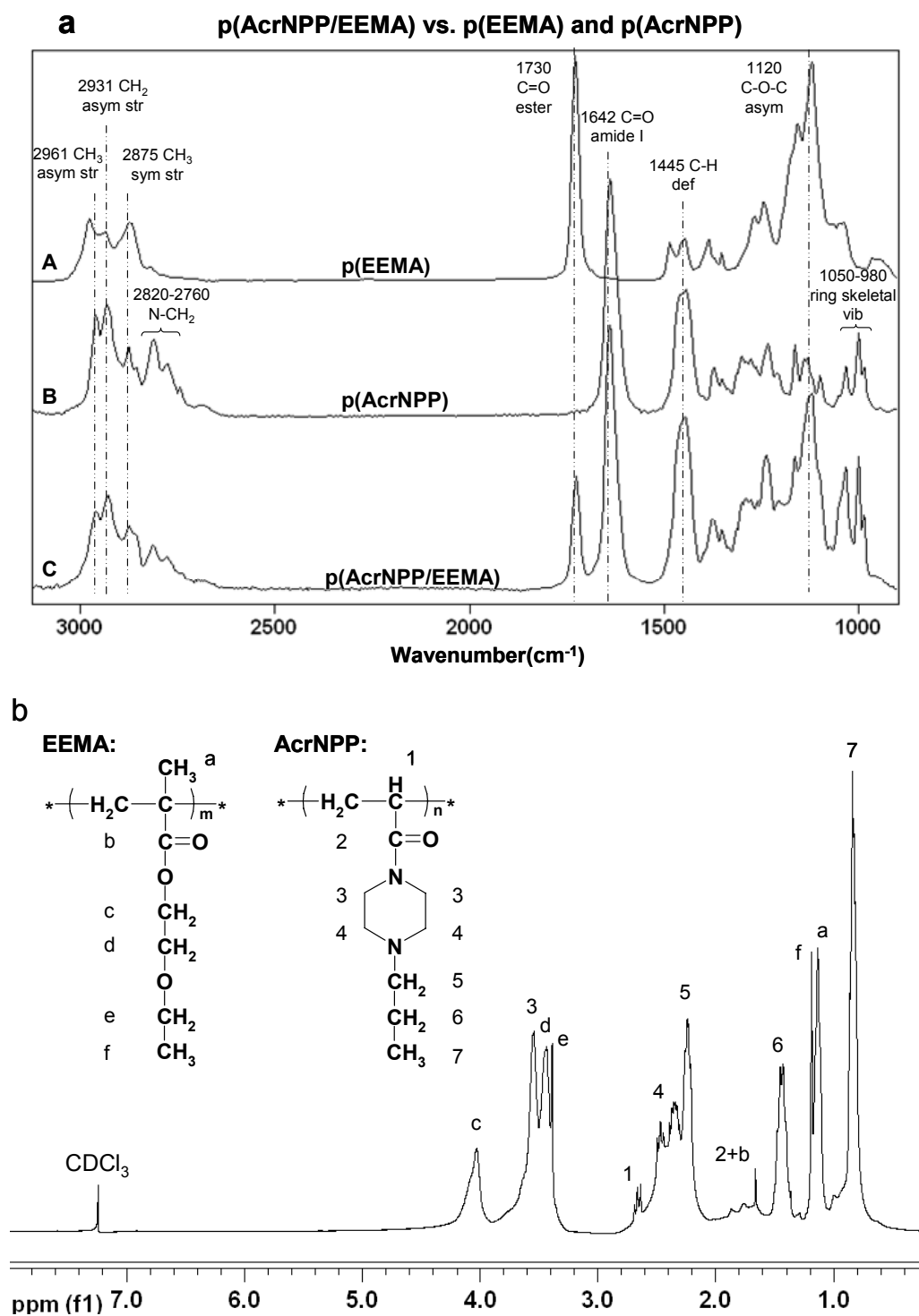


Figure S1. (a) ATR FT-IR spectra of: A – p(EEMA); B – p(AcrNPP); C – p(AcrNPP/EEMA); and (b) ^1H NMR spectrum of p(AcrNPP/EEMA) in CDCl_3 .

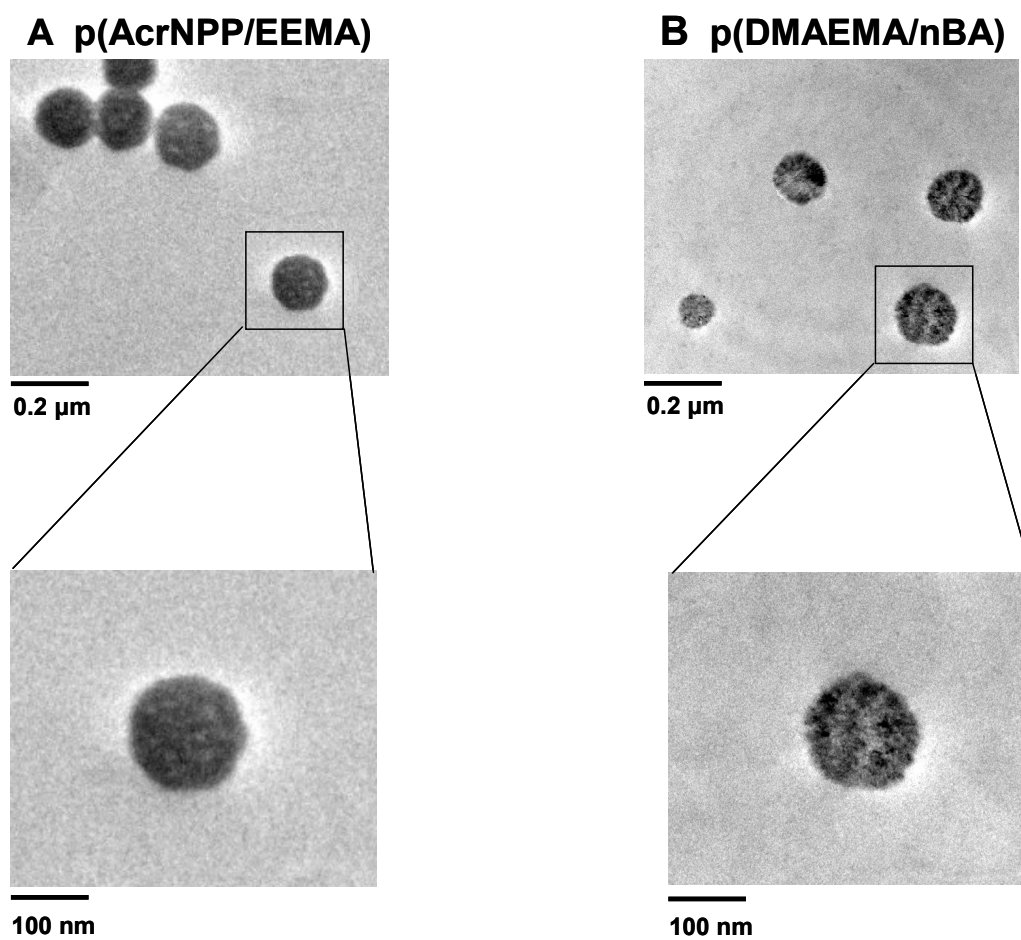


Figure S2. TEM images of p(AcrNPP/EEMA) (A) and p(DMAEMA/nBA) (B) colloidal particles.

Reference

1. Tiemblo, P.; Laguna, M. F.; Garcia, F.; Garcia, J. M.; Riande, E.; Guzman, J. *Macromolecules* 2004, 37, 4156.
2. Sanmathi, C. S.; Prasannakumar, S.; Sherigara, B. S. *Bull. Mater. Sci* 2004, 27, 243.
3. Gan, L. H.; Gan, Y. Y.; Deen, R. *Macromolecules* 2000, 33, 7893.
4. Coskun, M.; Barim, G.; Demirelli, K. *J. Macromol. Sci., Pure Appl. Chem.* 2006, 43, 83.
5. Chang, L.; Kong, X.; Wang, F.; Wang, L.; Shen, J. *Thin Solid Films* 2008, 516, 2125.
6. Lin-Vien, D.; Colthup, N. B.; Fateley, W. G.; Grasselli, J. G., *The Handbook of Infrared and Raman Characteristic Frequencies of Organic Molecules*. Academic Press: San Diego, 1991.
7. Pretsch, E.; Bühlmann, P.; Affolter, C., *Structure Determination of Organic Compounds: Tables of Spectral Data*. 3rd ed.; Springer: New York, 2000.
8. Socrates, G., *Infrared and Raman Characteristic Group Frequencies: Tables and Charts*. 3rd ed.; John Wiley and Sons Ltd: New York, 2001.